

X-ray bright sources in the *Chandra* Small Magellanic Cloud Wing Survey – detection of two new pulsars

K. E. McGowan,^{1*} M. J. Coe,¹ M. Schurch,¹ V. A. McBride,¹ J. L. Galache,²
W. R. T. Edge,¹ R. H. D. Corbet,³ S. Laycock,² A. Udalski⁴ and D. A. H. Buckley^{5,6}

¹*School of Physics and Astronomy, Southampton University, Highfield, Southampton SO17 1BJ*

²*Harvard–Smithsonian Center for Astrophysics, Cambridge, MA 02138, USA*

³*Universities Space Research Association, X-ray Astrophysics Laboratory, Mail Code 662, NASA Goddard Space Flight Center, Greenbelt, MD 20771, USA*

⁴*Warsaw University Observatory, Aleje Ujazdowskie 4, 00-478 Warsaw, Poland*

⁵*South African Astronomical Observatory, Observatory, 7935 Cape Town, South Africa*

⁶*Southern African Large Telescope Foundation, Observatory, 7935 Cape Town, South Africa*

Accepted 2007 January 4. Received 2007 January 3; in original form 2006 November 6

ABSTRACT

We investigate the X-ray and optical properties of a sample of X-ray bright sources from the Small Magellanic Cloud (SMC) Wing Survey. We have detected two new pulsars with pulse periods of 65.8 s (CXOU J010712.6–723533) and 700 s (CXOU J010206.6–714115), and present observations of two previously known pulsars RX J0057.3–7325 (SXP101) and SAX J0103.2–7209 (SXP348). Our analysis has led to three new optical identifications for the detected pulsars. We find long-term optical periods for two of the pulsars, CXOU J010206.6–714115 and SXP101, of 267 and 21.9 d, respectively. Spectral analysis of a subset of the sample shows that the pulsars have harder spectra than the other sources detected. By employing a quantile-based colour–colour analysis we are able to separate the detected pulsars from the rest of the sample. Using archival catalogues we have been able to identify counterparts for the majority of the sources in our sample. Combining this with our results from the temporal analysis of the *Chandra* data and archival optical data, the X-ray spectral analysis, and by determining the X-ray to optical flux ratios we present preliminary classifications for the sources. In addition to the four detected pulsars, our sample includes two candidate foreground stars, 12 probable active galactic nuclei, and five unclassified sources.

Key words: X-rays: binaries – stars: emission-line, Be – Magellanic Clouds.

1 INTRODUCTION

The Small Magellanic Cloud (SMC) is turning out to be an exciting nest of X-ray binary pulsars. Estimates of the star formation rate (SFR) for the SMC range between $0.044 M_{\odot} \text{ yr}^{-1}$ from $H\alpha$ measurements (Kennicutt 1991) to $0.38 M_{\odot} \text{ yr}^{-1}$ from supernova birth rates (Filipovic et al. 1998). Using the relation between the X-ray luminosity function of high-mass X-ray binaries (HMXBs) and the SFR of the host galaxy (Grimm, Gilfanov & Sunyaev 2003) and the upper and lower SFR estimates, Shtykovskiy & Gilfanov (2005) predict between 6 and 49 HMXBs with luminosities $\geq 10^{35} \text{ erg s}^{-1}$ in the SMC. We now know of ~ 50 such systems in the SMC (Haberl & Pietsch 2004; Coe et al. 2005).

Several of these detections have come from *Chandra* and *RXTE* work over the last couple of years (Edge et al. 2004; Laycock et al. 2005). This large number suggests a dramatic phase of star birth in

the past, probably associated with the most recent closest approach between the SMC and the Large Magellanic Cloud (LMC; Gardiner & Noguchi 1996). Even more extreme, Nazé et al. (2003) analysed a ~ 100 ks exposure of just one 20×20 arcmin² *Chandra* field and identified more than 20 probable Be/X-ray binary systems. Multiplying these numbers up by the $\sim 2 \times 2$ -deg² size of the SMC, and allowing for ~ 10 per cent X-ray duty cycles, suggests the final number of Be/X-ray binaries could be well in excess of 1000. Thus the study of the SMC is not only providing a great homogeneous sample of HMXBs for study, but is also providing direct insights into the history of our neighbouring galaxy.

It is important to note that, despite appearances, the SMC is a very three dimensional object. Studies of the Cepheid population by Laney & Stobie (1986) have revealed that the depth of the SMC is up to 10 times its observed width. The two main structures, the Bar and the Wing, lie ~ 11 kpc behind, and ~ 8 kpc in front of the main body of the SMC, respectively.

To date most of the X-ray studies by *Chandra* and *RXTE* have concentrated on the Bar which has proved to be a large source of

*E-mail: kem@astro.soton.ac.uk

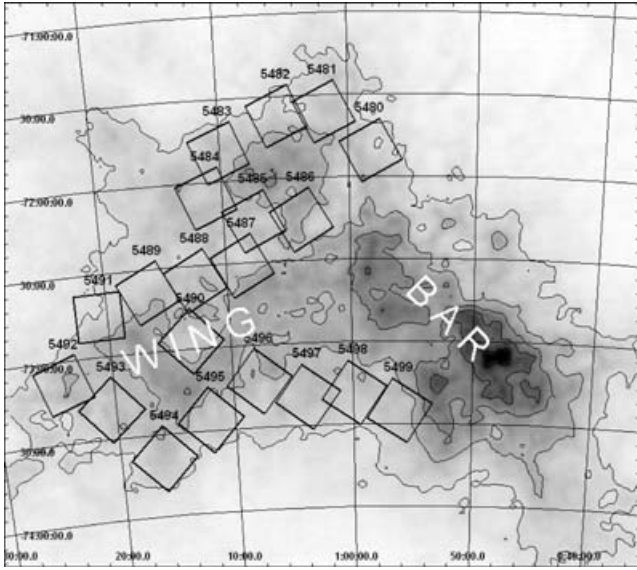


Figure 1. The location of the 20 fields studied by *Chandra* in this work, overlaid on a neutral hydrogen density image of the SMC (Stanimirović et al. 1999). The Wing and Bar of the SMC are marked.

HMXBs. The *Chandra* work presented here focuses on a study of the Wing of the SMC. Its intention is to compare the pulsar population of the Wing with what we already know for the Bar. Coe et al. (2005) studied the locations of the detected X-ray pulsars and believed they identified a relationship between the H I intensity distribution and that of the pulsars. They found that the pulsars seem to lie in regions of low/medium H I densities, suggesting that high-mass star formation is well suited to these densities. The locations of the *Chandra* observations reported here are based upon this analysis.

Table 1. X-ray bright sources in the SMC Wing Survey.

Object	Name	RA (J2000)	Dec. (J2000)	Error (arcsec)	Counts	P_{pulse} (s)	Pulsed fraction (per cent)	Observation ID	Date
1	CXOU J005551.5–733110	00:55:51.54	–73:31:10.1	0.88	231	–	–	5499	2006-03-03
2	RX J0057.3–7325	00:57:27.08	–73:25:19.5	0.83	433	101.16	29 ± 7	5499	2006-03-03
3	CXOU J005754.4–715630	00:57:54.41	–71:56:30.9	0.95	130	–	–	5480	2006-02-06
4	CXOU J010014.2–730725	01:00:14.22	–73:07:25.3	1.88	110	–	–	5498	2006-03-03
5	CXOU J010206.6–714115	01:02:06.69	–71:41:15.8	0.83	383	700.54	35 ± 9	5481	2006-02-06
6	CXOU J010245.0–721521	01:02:45.01	–72:15:21.7	0.91	81	–	–	5486	2006-02-10
7	SAX J0103.2–7209	01:03:13.94	–72:09:14.4	0.90	244	337.51	45 ± 19	5486	2006-02-10
8	CXOU J010455.4–732555	01:04:55.50	–73:25:55.2	1.33	58	–	–	5497	2006-03-03
9	CXOU J010509.6–721146	01:05:09.68	–72:11:46.6	1.17	50	–	–	5486	2006-02-10
10	CXOU J010533.0–721331	01:05:33.08	–72:13:31.2	1.21	80	–	–	5486	2006-02-10
11	CXOU J010712.6–723533	01:07:12.63	–72:35:33.8	0.87	1919	65.78	37 ± 5	5487	2006-02-10
12	CXOU J010735.0–732022	01:07:35.00	–73:20:22.6	1.20	66	–	–	5496	2006-03-03
13	CXOU J010836.6–722501	01:08:36.65	–72:25:01.7	0.99	67	–	–	5487	2006-02-10
14	CXOU J010849.5–721232	01:08:49.51	–72:12:32.9	0.90	144	–	–	5485	2006-02-08
15	CXOU J010855.6–721328	01:08:55.64	–72:13:28.2	1.02	54	–	–	5485	2006-02-08
16	CXOU J011021.3–715201	01:10:21.31	–71:52:01.2	0.80	94	–	–	5483	2006-02-06
17	CXOU J011050.6–721025	01:10:50.62	–72:10:25.9	0.92	82	–	–	5484	2006-02-06
18	CXOU J011154.2–723105	01:11:54.28	–72:31:05.0	0.92	82	–	–	5488	2006-02-12
19	CXOU J011303.4–724648	01:13:03.46	–72:46:48.4	1.83	86	–	–	5490	2006-02-27
20	CXOU J011744.7–733922	01:17:44.77	–73:39:22.7	0.96	89	–	–	5494	2006-03-01
21	CXOU J011832.4–731741	01:18:32.44	–73:17:41.6	1.40	71	–	–	5493	2006-02-27
22	CXOU J012027.3–724624	01:20:27.31	–72:46:24.8	0.78	64	–	–	5491	2005-07-24
23	CXOU J012223.6–730848	01:22:23.65	–73:08:48.5	0.96	301	–	–	5492	2005-08-12

2 THE *CHANDRA* SMC WING SURVEY

We performed a survey with *Chandra* of the wings of the SMC between 2005 July and 2006 March (see Fig. 1). A total of 20 fields were observed using the standard ACIS-I imaging mode configuration which utilizes chips I0–I3 plus S2 and S3. The exposure times for each field ranged from 8.6–10.3 ks. We performed the data reduction using CIAO v3.2. The event files were filtered to restrict the energy range to 0.5–8.0 keV and we barycentrically corrected the data. Potential sources were detected using the wavdetect algorithm. Here we present the analysis of the 23 brightest X-ray sources (>50 counts) in the survey (see Table 1). The positional errors quoted are the 95 per cent confidence region for the source position that takes into account the properties of the telescope optics and the source brightness (see Hong et al. 2005), combined in quadrature with the boresight error (~ 0.7 arcsec at 95 per cent confidence). A full analysis and catalogue of sources from all 20 fields will be presented in a future publication (McGowan et al., in preparation).

2.1 Temporal analysis

The main goal of the SMC Wing Survey is to detect new pulsars. We created background subtracted light curves for the 23 sources in our sample and searched for periodic variations from 6.5–1000 s. The temporal analysis was performed using the Starlink PERIOD software and we generated Lomb–Scargle and phase dispersion minimization periodograms for each of our sources.

We determined the 90 and 99 per cent confidence levels for the Lomb–Scargle periodograms from a cumulative probability distribution appropriate for each data set. Using a Monte Carlo method we generated 10 000 simulated light curves with the same time sampling and variance as the real data. The simulated light curves were taken from a Gaussian distribution. A Lomb–Scargle periodogram was produced for each simulated light curve, and the peak power

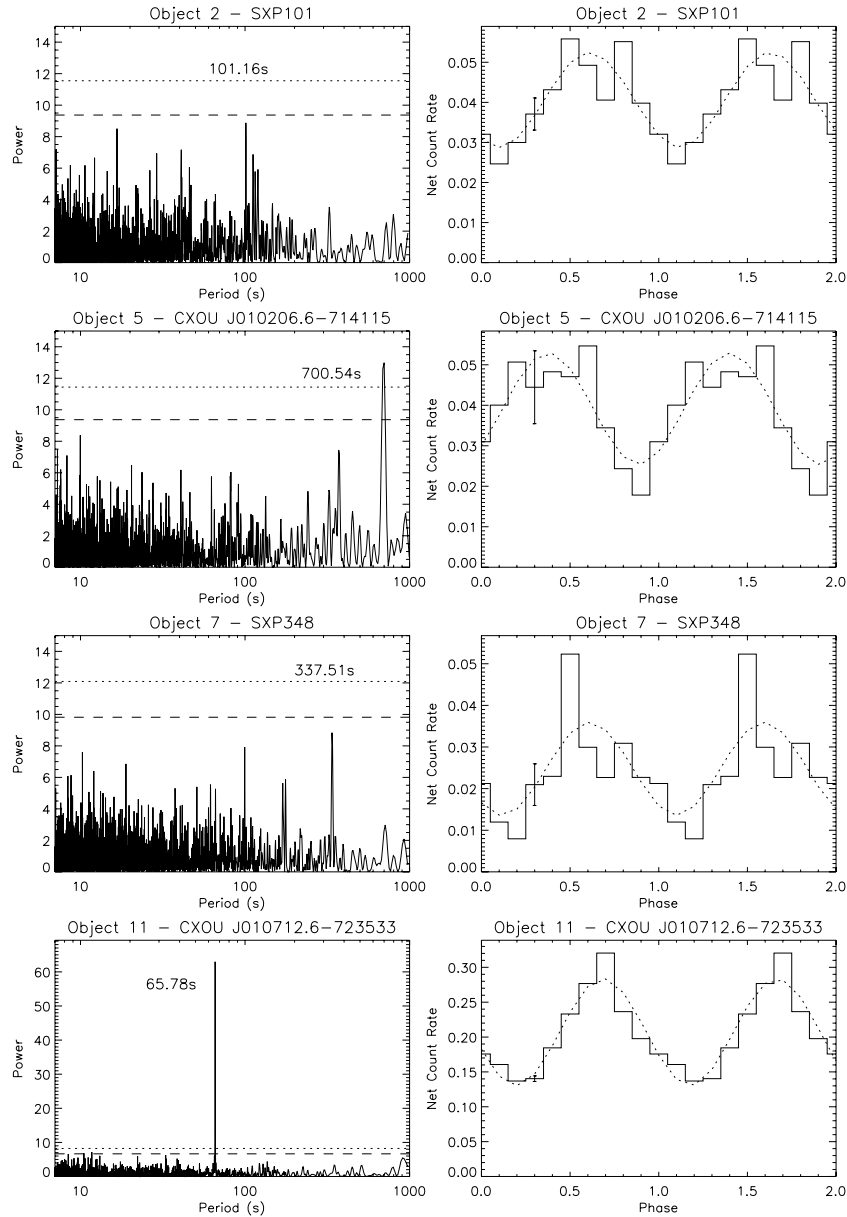


Figure 2. Temporal analysis of the *Chandra* data. Left-hand panels: Lomb–Scargle periodograms for the sources where a significant peak was detected. The 90 per cent (dashed line) and 99 per cent (dotted line) confidence limits are shown. Right-hand panels: the pulse profiles for the sources with error bars, where the uncertainty is the standard error for the data points in the bin. The fitted sine functions are shown (dotted line).

was recorded. From these values the probability of obtaining a given peak power from pure noise can be calculated and the cumulative distribution function derived.

Two sources show a significant peak in the Lomb–Scargle periodogram and a corresponding strong peak in the phase dispersion minimization periodogram. Two of the other sources in the sample are the previously known pulsars, RX J0057.3–7325 = SXP101 and SAX J0103.2–7209 = SXP348. These two show pulsations, but at a level below the 90 per cent confidence limit. The power spectra for all four sources are shown in Fig. 2 (left-hand panels). We folded the light curves on the detected periods (see Fig. 2, right-hand panels) and fitted the resulting pulse profiles with a sine function to determine the pulsed fractions (see Table 1). We define the pulse fraction as $(F_{\max} - F_{\min}) / (F_{\max} + F_{\min})$, where F_{\max} and F_{\min} are the maximum and minimum of the fitted pulse light curve.

The error on the periods were determined using Kovács formula (Kovács 1981; Horne & Baliunas 1986). Using this method the uncertainty calculated takes into account both the resolution due to the light-curve sampling and the signal-to-noise ratio of the detected modulation.

2.2 Spectral analysis

We have extracted spectra for the sources with >100 counts using CIAO v3.2 tools. The spectra were regrouped by requiring at least 10 counts per spectral bin for the brighter sources (>200 counts), and 2 counts per bin for the fainter sources ($100 < \text{counts} < 200$). The subsequent spectral fitting and analysis were performed using XSPEC v12.3.0. We fitted each spectrum with a power law, thermal bremsstrahlung and Mekeal model. In each fit we included

Table 2. Spectral fits to the X-ray bright sources in the SMC Wing Survey.

Object	Model	Γ	T (10^6 K)	ΔC (d.o.f.)	f_X ($\text{erg cm}^{-2} \text{s}^{-1}$)
1	PL	$1.9^{+0.2}_{-0.2}$	–	0.5 (20)	3.3×10^{-13}
	Brem	–	$41.0^{+20.5}_{-12.0}$	0.4 (20)	2.7×10^{-13}
	Mekal	–	$49.4^{+20.0}_{-11.9}$	0.6 (20)	2.9×10^{-13}
2	PL	$0.6^{+0.1}_{-0.1}$	–	1.0 (35)	1.0×10^{-12}
	Brem	–	2314	2.3 (35)	7.5×10^{-13}
	Mekal	–	927	2.5 (35)	7.2×10^{-13}
3	PL	$1.3^{+0.2}_{-0.2}$	–	1.1 (55)	2.5×10^{-13}
	Brem	–	273 ± 192	1.1 (55)	2.3×10^{-13}
	Mekal	–	270 ± 188	1.1 (55)	2.4×10^{-13}
4	PL	$3.4^{+0.4}_{-0.4}$	–	0.8 (45)	3.6×10^{-13}
	Brem	–	$7.3^{+2.8}_{-1.4}$	0.8 (45)	2.1×10^{-13}
	Mekal	–	$14.9^{+1.6}_{-3.4}$	1.4 (45)	1.2×10^{-13}
5	PL	$0.4^{+0.1}_{-0.1}$	–	0.8 (34)	1.4×10^{-12}
	Brem	–	2314	3.2 (34)	8.5×10^{-13}
	Mekal	–	927	3.6 (34)	8.2×10^{-13}
7	PL	$0.8^{+0.2}_{-0.2}$	–	1.4 (21)	5.8×10^{-13}
	Brem	–	2314	2.0 (21)	4.5×10^{-13}
	Mekal	–	927	2.2 (21)	4.6×10^{-13}
11	PL	$0.3^{+0.1}_{-0.1}$	–	1.1 (159)	7.1×10^{-12}
	PL ^a	$0.5^{+0.1}_{-0.1}$	–	1.1 (158)	6.9×10^{-12}
	Brem	–	2314	4.4 (159)	4.0×10^{-12}
14	Mekal	–	927	4.8 (159)	4.4×10^{-12}
	PL	$1.7^{+0.2}_{-0.2}$	–	1.1 (59)	2.4×10^{-13}
	Brem	–	133.4	2.0 (59)	2.1×10^{-13}
23	Mekal	–	$74.1^{+88.5}_{-27.2}$	1.1 (59)	2.3×10^{-13}
	PL	$1.5^{+0.2}_{-0.2}$	–	0.8 (105)	5.2×10^{-13}
	Brem	–	$109.3^{+129.9}_{-41.8}$	0.8 (105)	4.6×10^{-13}
	Mekal	–	$105.1^{+172.2}_{-39.0}$	0.9 (105)	4.9×10^{-13}

The data were fitted with absorbed power law (PL), bremsstrahlung (Brem) and Mekal models, assuming a neutral hydrogen column density of $N_{\text{H}} = 0.06 \times 10^{22} \text{ cm}^{-2}$, where Γ is the photon index and T is the temperature determined from the fits. The goodness of fit using the C-statistic (ΔC) and the unabsorbed flux in the 0.3–10 keV range are also given.^aModel fit results in $N_{\text{H}} = 0.19^{+0.09}_{-0.08} \times 10^{22} \text{ cm}^{-2}$.

absorption. Due to the low number of counts detected we fixed the column density at the value for the SMC of $6 \times 10^{20} \text{ cm}^{-2}$, only in the case of source #11 (CXOU J010712.6–723533) have we also allowed the N_{H} to be fit. The small number of detected counts renders chi-squared statistics invalid. We have therefore used an alternative statistic, the C-statistic (Cash 1979), for our model fitting. The goodness of fit given in Table 2, ΔC , is determined in a similar way to reduced χ^2 . The unabsorbed flux in the 0.3–10 keV band has been determined for each fit. For sources that are members of the SMC, or assumed members (see Section 2.4), we have also calculated the luminosity in the 0.3–10 keV range, using a distance to the SMC of 60 kpc (based on the distance modulus Westerlund (1997)). The results of the spectral fitting are summarized in Table 2.

2.3 Long-term optical light curves

All 23 objects were investigated for possible optical periods (see Table 3). Such periods have been found in many previous HMXB systems in the SMC and can either represent the binary period of the system or non-radial pulsations (NRPs) from the mass-donor star (for examples of both see Edge et al. 2005; Schmidtke &

Cowley 2006). Data were collected from as many of the following possible sources: OGLE II (Udalski, Kubiak & Szymański 1997; Szymański 2005), OGLE III and MACHO (Alcock et al. 1999). The OGLE III archive contains *I*-band photometry spanning 5 yr, the data are not yet public. In each case the optical light curves were searched for periods in the ranges 10–1000 d and 1–10 d by generating Lomb–Scargle periodograms. If a significant period was found, then the data were folded modulo that period with phase zero set to the time of maximum light phase. In one case (source #5, CXOU J010206.6–714115) the data were first detrended with a polynomial fit. Quite a few of the objects revealed long-term variations on time-scales of 100–1000 d – such changes are similar to the common Type 4 variations reported by Mennickent et al. (2002) from Be stars in the SMC. The errors on the periods were determined using the same method as for the pulse periods (see Section 2.1).

2.4 X-ray to optical flux ratios

Using the results from the spectral fitting and information from optical catalogues we have constructed X-ray to optical flux ratios for the majority of the sources in our sample (Table 4). It has been shown that such ratios are a good discriminator for different classes of sources (see e.g. Maccacaro et al. 1988; Hornschemeier et al. 2001), with typical values for active galactic nuclei (AGNs) lying in the region $\log(f_X/f_{\text{opt}}) = 0.0 \pm 1$. We have used the flux in the 0.5–2 keV band and equation (3) from Hornschemeier et al. (2001) to calculate the ratio for each source that has a measured *R* magnitude. In the case of a source that has too few counts to model in XSPEC, we have determined the flux given the count rate and assuming a power-law index of 1.6 (see Section 4) and neutral hydrogen column density of $6 \times 10^{20} \text{ cm}^{-2}$, using PIMMS v3.9a. The results of this analysis allow us to provisionally classify the sources and determine whether the object is a member of the SMC (see Section 3).

2.5 Quantile analysis

We have used the quantile analysis technique of Hong, Schlegel & Grindlay (2004) to investigate the X-ray colours of the 23 sources in our sample. In a traditional hardness ratio the photons are split into predefined energy bands. The quantile method divides the photon distribution into a given number of equal proportions, where the quantiles are the energy values that mark the boundaries between consecutive subsets. This has the advantage, compared to traditional hardness ratios, that there is no spectral dependence and a colour can be calculated even for sources with very few counts (for more details see Hong et al. 2004).

For each source we determine the median and quartiles of the photon energy distribution. In Fig. 3 we show the quantile-based colour–colour diagram (QCCD), using the median and the ratio of two quartiles, for our sample. In the diagram the spectrum hardens as one goes further towards right-hand side and changes from concave-downward to concave-upward moving from top to bottom (see fig. 7, Hong et al. 2004). We have included in the figure the pulsars detected by Edge et al. (2004). The new and known pulsars are marked.

3 INDIVIDUAL SOURCES

3.1 CXOU J005551.5–733110

This source was detected in observation ID 5499 taken on 2006 March 3 (MJD 53797). The temporal analysis does not reveal any

Table 3. Optical counterparts for the X-ray bright sources in the SMC Wing Survey.

Object	OGLE III	Optical counterpart OGLE II	MACHO	Period (d)	Comment
1	SMC106.8 21521			–	Changes of ~ 0.1 mag over ~ 400 d
2	SMC106.7 15343		211.16415.11	21.9	SXP101. Optical period seen in both OGLE III and MACHO data
3	SMC108.4 384			–	Some variability (~ 0.1 mag) on time-scales of ~ 100 d
4			211.16591.6	29.6	MACHO data only, saturated in OGLE III. Period is not strong in MACHO and affected by many saturated points
5	SMC114.7 39			267	New pulsar, CXOU J010206.6–714115. Overall brightness change of 0.5 mag over ~ 1000 d
6		SMC-SC9 168928	206.16775.520	–	No variability
7		SMC-SC9 173121	206.16776.17	–	SXP348. Variability (~ 0.1 mag) on time-scales of ~ 400 d
8	SMC111.7 8943			1.49	Sinusoidal folded light curve of 0.04 mag amplitude
9	SMC113.2 13190		206.16947.35	–	No variability
10	SMC113.2 13509		206.16946.1089	–	No variability
11		SMC-SC11 48835	206.17055.21	–	New pulsar, CXOU J010712.6–723533. Brightening of ~ 0.02 mag over ~ 1200 d
12	?			?	Not in OGLE or MACHO fields
13	SMC113.1 9719	SMC-SC11 116013	206.17114.1658	–	Brightening of ~ 0.5 mag over ~ 800 d
14	SMC118.7 galaxy	SMC-SC11 120966	206.17175.739	–	No variability
15	SMC118.7 galaxy		206.17174.524	–	No variability
16	SMC118.5 1160			–	Some variability (~ 0.2 mag) on time-scales of ~ 100 d
17	SMC118.7 10314			–	No variability
18	SMC115.5 12842			–	No variability
19	SMC115.7 18128			–	Brightening of ~ 0.4 mag in ~ 1500 d
20	SMC117.4 3274			–	Brightening of ~ 0.4 mag in ~ 1000 d
21	SMC121.6 galaxy			?	Galaxy
22	SMC120.7 6336			–	No variability
23	SMC121.4 542			–	No variability

significant periodicities. The location of CXOU J005551.5–733110 is close to source 65 in the *ROSAT* HRI catalogue of the SMC (Sasaki, Haberl & Pietsch 2000), being consistent within errors. The position of the *Chandra* source coincides with 2MASS 00555147–7331101 ($J = 16.3$, $H = 15.4$, $K = 14.6$) and OGLE III source SMC106.8 21521 ($I = 17.7$). The optical light curve displays changes of ~ 0.1 mag over ~ 400 d. The X-ray emission from the source is well fitted by a thermal bremsstrahlung with a temperature of 4.1×10^7 K, however the temperature is poorly constrained (see Table 2). A power law also fits the data well with an index of 1.9. If this source is a member of the SMC the unabsorbed luminosities derived from these fits are 1.2×10^{35} and 1.4×10^{35} erg s $^{-1}$, respectively.

3.2 RX J0057.3–7325 = SXP101

RX J0057.3–7325 = AX J0057.4–7325 (Kahabka et al. 1999; Torii et al. 2000), also known as SXP101 (Coe et al. 2005), was detected in observation ID 5499 taken on 2006 March 3 (MJD 53797). Coherent pulsations with a period of 101.45 ± 0.07 s were detected in ASCA data (Torii et al. 2000). The strongest peak in both period searches of the *Chandra* data occurs at 101.16 ± 0.86 s (see Fig. 2), however the peak in the Lomb–Scargle falls below the <90 per cent confidence level and would not have been regarded as significant if the source was not already known.

Edge & Coe (2003) narrowed the optical counterpart down to two sources, D and E in Table 2 in their paper. Our more precise *Chandra* position allows us to determine that the optical counterpart is source E, Table 2 in Edge & Coe (2003), the star MACS J0057–734 10 (Tucholke, De Boer & Seitter 1996). This position is also consistent with 2MASS 00572706–7325192 ($J = 15.7$, $H = 15.6$, $K = 15.6$), MACHO object 211.16415.11 ($V = 14.9$, $R = 14.8$) and OGLE III source SMC106.7 15343 ($I = 15.6$). We find a period of 21.94 ± 0.10 d in both the OGLE III and MACHO data (Fig. 4). From the Corbet diagram (Corbet 1986) we would expect a longer period for the source, perhaps twice the detected period, however there are no strong peaks in that region of the periodogram. A period of 22.95 d is found in the X-ray data from *RXTE* with $T_0 =$ MJD 2452111.4 (Galache et al., in preparation). The spectrum of SXP101 is described well by a power law with a photon index of 0.6. The resulting unabsorbed luminosity is 4.3×10^{35} erg s $^{-1}$.

3.3 CXOU J005754.4–715630

This source was detected in observation ID 5480 taken on 2006 February 6 (MJD 53772). The temporal analysis does not reveal any significant periodicities. Within errors the position of CXOU J005754.4–715630 is consistent with USNO-B1.00180–0037995 ($B_2 = 19.2$, $R_2 = 20.1$), 2MASS J00575428–7156306 ($J = 16.8$, $H = 16.4$, $K = 14.8$) and OGLE III source SMC108.4 384 ($I = 18.5$).

Table 4. X-ray to optical flux ratios.

Object	R	f_X	$\log(f_X/f_R)$	Class
1	–	1.3×10^{-13}	–	–
2	14.8	1.0×10^{-13}	–1.58	Pulsar
3	20.1	8.3×10^{-14}	0.46	AGNs
4	10.9	1.3×10^{-13}	–3.03	Star
5	15.1	9.7×10^{-14}	–1.47	Pulsar
6	18.0	3.2×10^{-14}	–0.79	AGNs
7	13.3	6.8×10^{-14}	–2.34	Pulsar
8	14.5	2.8×10^{-14}	–2.25	Star
9	18.0	2.0×10^{-14}	–1.00	–
10	18.7	3.2×10^{-14}	–0.51	AGNs
11	14.9	4.4×10^{-13}	–0.90	Pulsar
12	–	2.8×10^{-14}	–	–
13	18.5	2.8×10^{-14}	–0.65	AGNs
14	19.4	7.7×10^{-14}	0.15	AGNs
15	18.9	2.0×10^{-14}	–0.64	AGNs
16	19.0	4.0×10^{-14}	–0.30	AGNs
17	–	3.6×10^{-14}	–	AGNs
18	19.3	3.2×10^{-14}	–0.27	AGNs
19	–	3.2×10^{-14}	–	–
20	19.6	3.6×10^{-14}	–0.10	AGNs
21	–	2.8×10^{-14}	–	AGNs
22	–	2.8×10^{-14}	–	–
23	19.1	1.4×10^{-13}	0.29	AGNs

f_X is the unabsorbed flux in the 0.5–2 keV range. The X-ray to optical flux ratio is determined using $\log(f_X/f_R) = \log f_X + 5.50 + R/2.5$ (equation 3, Hornschemeier et al. 2001).

The OGLE III light curve displays slight variation (~ 0.1 mag) on time-scales of ~ 100 d. The X-ray spectrum can be well fitted with a power law with photon index of 1.3. Statistically the data are equally well fitted with the thermal models, however the models are very poorly constrained (see Table 2). The X-ray to optical flux ratio for this source implies that it is a background AGN.

3.4 CXOU J010014.2–730725

This source was detected in observation ID 5498 taken on 2006 March 3 (MJD 53797). The temporal analysis does not reveal any significant periodicities.

The position of CXOU J010014.2–730725 is close to the previously detected source RX J0100.2–7307 (Kahabka et al. 1999) and source 86 in the *ROSAT* HRI catalogue of the SMC (Sasaki et al. 2000). The archival source has a 90 per cent confidence positional uncertainty of 10 arcsec which encompasses the *Chandra* position making it probable that they are the same source. Sasaki et al. (2000) made a tentative classification of the source as a foreground star. The counterpart to CXOU J010014.2–730725 is ISO-MCMS J010014.0–730725 detected by the *Infrared Space Observatory* and has been classified as a long-period red variable (Cioni et al. 2003). The source position is also consistent with 2MASS 01001398–7307253 ($J = 10.9$, $H = 10.2$, $K = 10.0$) and MACHO source 211.16591.6 ($V = 12.2$, $R = 10.9$). The source is saturated in the OGLE III data. Cioni et al. (2003) analysed the MACHO data for periodicities. The blue light curve was considered of poor quality. The red light curve was found to have a period of 29 d. We have analysed the MACHO data, after removing all the saturated points we find a weak period at 29.57 ± 0.35 d in the red band (Fig. 5). A larger peak at 367 ± 10 d is too close to one year to be considered as astrophysical in origin.

The X-ray emission from CXOU J010014.2–730725 is very soft with almost no photons above ~ 2 keV. The spectrum can be well fitted with a power law with index of 3.4 or a thermal bremsstrahlung with temperature 7.3×10^6 K (see Table 2). The position of the source in the QCCD suggests that it is a stellar coronal emission source (Hong et al. 2005). Assuming this is the case, the X-ray to optical ratio based on the thermal fit is consistent with a galactic source. The $V - R$ colour for the source is 1.3, consistent with an M star (M0–M2), as are the infrared colours. We classify CXOU J010014.2–730725 as a foreground star.

3.5 CXOU J010206.6–714115

Observation ID 5481 took place on 2006 February 6 (MJD 53772). Timing analysis of this object revealed a period of 700.54 ± 34.53 s with a confidence of >99 per cent (see Fig. 2). The data were examined to ensure that this periodicity was not an artefact of the 707 s Z dithering frequency.

The position of this pulsar coincides with the emission-line star [MA93] 1301 (Meyssonnier & Azzopardi 1993), the $V = 14.6$ mag O9 star AzV 294 (Massey 2002), the OGLE III object SMC114.7 39 ($I = 14.3$), and 2MASS J01020668–7141161 ($J = 14.2$, $H = 14.0$, $K = 13.9$). The $B - V$ colour index is -0.14 (Massey 2002) which is consistent with the value expected from the optical companion of a Be X-ray binary. The OGLE III light curve shows a strong period at 267.38 ± 15.10 d (Fig. 6). This period is consistent with that predicted from the Corbet diagram (Corbet 1986) for a 700 s Be/X-ray pulsar (following the convention of Coe et al. 2005 this source would be designated SXP700).

The X-ray spectrum of CXOU J010206.6–714115 can be well fitted with a power law with index of 0.4 (see Table 2). This model implies an unabsorbed luminosity of 6.0×10^{35} erg s $^{-1}$.

3.6 CXOU J010245.0–721521

This source was detected in observation ID 5486 taken on 2006 February 10 (MJD 53776). The position of CXOU J010245.0–721521 is consistent with OGLE II SMC-SC9 168928 ($B = 19.4$, $V = 18.9$ and $I = 18.4$), a known quasar at $z = 1.06$ (Dobrzycki et al. 2003). The source is also detected by MACHO and is designated 206.16775.520 ($V = 18.9$, $R = 18.0$). The optical light curves do not show any variability. The position of the source on the QCCD indicates that the classification as a quasar is correct and the X-ray to optical flux ratio is consistent with a background AGN.

3.7 SAX J0103.2–7209 = SXP348

SAX J0103.2–7209 = 2E 0101.5–7225 = RX J0103.2–7209 was first identified by *BeppoSAX* in 1998 (Israel et al. 1998) and showed pulsations at a period of 345.2 ± 0.1 s. The source, also known as SXP348 (Coe et al. 2005), was also seen in *ASCA* data taken in 1996, with a reported pulse period of 348.9 ± 0.3 s and period derivative (with respect to *BeppoSAX*) of 1.7 s yr $^{-1}$ (Yokogawa & Koyama 1998). The pulse period determined from observations taken in 1999 with *Chandra* of 343.5 ± 0.5 s indicated that the pulsar had been spinning up with a constant rate since 1996 (Israel et al. 2000). Using serendipitous *XMM-Newton* observations of the source from 2000, Haberl & Pietsch (2004) measured a pulse period of 341.21 ± 0.50 s, implying that the spin-up was continuing.

We observed SXP348 on 2006 February 10 (MJD 53776). Although the highest peak in the Lomb–Scargle periodogram is at

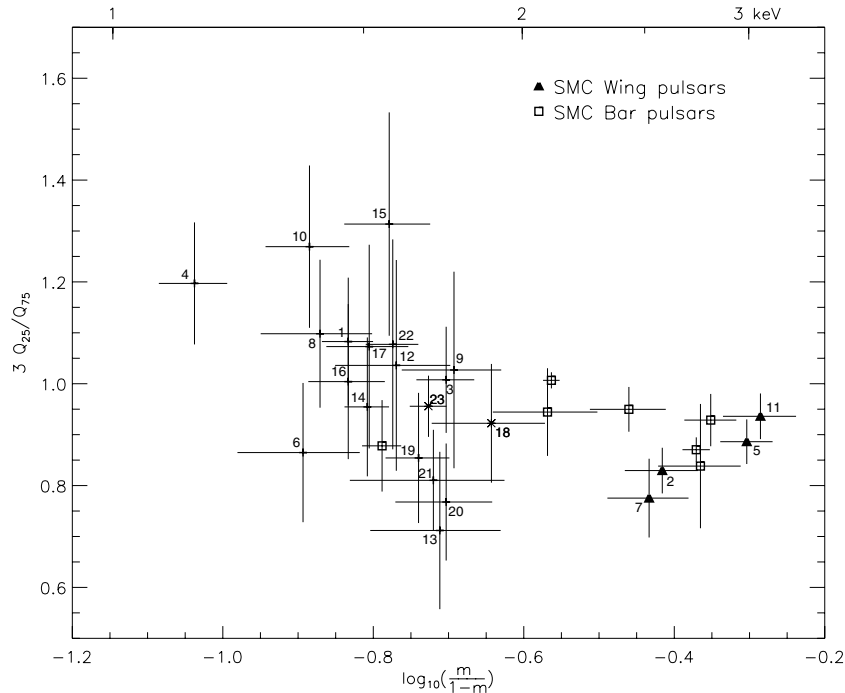


Figure 3. Quantile-based colour–colour diagram for the X-ray bright sources in the SMC Wing survey. The median and two quartiles of the photon energy distribution are given by m , Q_{25} and Q_{75} , respectively. The choice of x -axis allows the soft and hard phase space to be explored equally well (for more details see Hong et al. 2004). The new and known pulsars in the SMC Bar (open squares, Edge et al. 2004) and the SMC Wing (filled triangles) and marked. Source #6 is a known quasar, and source #4 is a probable variable star. The two sources marked with a cross are source #18 (CXOU J011154.2–723105) and source #23 (CXOU J012223.6–730848). Both of these sources display possible pulsations at 19.52 and 140.99 s, respectively, but their optical magnitudes and lack of long-term variability seems to rule out classification as Be/X-ray transients, and the nature of the sources are uncertain.

337.51 ± 5.17 s, it falls below the 90 per cent confidence limit (see Fig. 2). While our results seem to suggest that SXP348 may still be spinning up, due to the uncertainty on the spin period we are unable to determine if the previously observed trend is still persisting.

The pulsar has previously been identified with a $V = 14.8$ mag Be star (Hughes & Smith 1994; Israel et al. 1998), [MA93] 1367 (Meyssonnier & Azzopardi 1993). Coe & Orosz (2000) analysed OGLE II data of the proposed optical counterpart and concluded that it was the likely companion. Timing analysis of the long-term I -band OGLE II data did not show any periodic modulation in the range 1 to 50 d with an upper limit of $\leq \pm 0.02$ mag. The source position is also coincident with the MACHO object 206.16776.17 ($V = 14.4$, $R = 13.3$). Our analysis of the light curve does not reveal any coherent period in the range 1 to 1000 d. The source falls in a gap between the chips in OGLE III.

It has been shown that the spectrum of SXP348 can be well fitted with an absorbed power law with photon index ~ 1.0 (Israel et al. 1998; Yokogawa & Koyama 1998; Haberl & Pietsch 2004). We find that the X-ray emission is well fitted by a power law with index 0.8 (see Table 2). This fit gives an unabsorbed luminosity of 2.5×10^{35} erg s $^{-1}$.

3.8 CXOU J010455.4–732555

This source was detected in observation ID 5497 taken on 2006 March 3 (MJD 53797). The source is located very near to the edge of the chip and only falls on the chip for part of the observation. We were therefore unable to perform a search for pulsations.

The position of CXOU J010455.4–732555 is coincident with USNO-B1.00165–0046936 ($R1 = 14.5$, $B2 = 15.3$, $R2 = 15.0$),

2MASS 01045550–7325558 ($J = 12.4$, $H = 11.8$, $K = 11.8$) and OGLE III source SMC111.7 8943 ($I = 13.0$). The OGLE III light curve reveals a period of 1.4880 ± 0.0005 d (Fig. 7). The next largest peak is at 3.0238 d. It is unclear whether the true period is 1.4880 or 3.0238 d, however the values are not consistent with the shorter period being a harmonic of the longer one. The peak at ~ 3 d could be due to the beating of the true period with the 1-d sampling variation. If the source was a Be/X-ray binary it is hard to reconcile the detected variation with an orbital period; in this case it could be a NRP. However, the optical brightness of the object indicates that the source is likely to be a variable star. The results from the X-ray to optical flux ratio calculation are consistent with a Galactic foreground star. Further X-ray observations to search for pulsations and follow-up optical spectroscopy are needed to determine the nature of this source.

3.9 CXOU J010509.6–721146

This source was detected in observation ID 5486 taken on 2006 February 10 (MJD 53776). The temporal analysis does not reveal any significant periodicities. The location of CXOU J010509.6–721146 lies within the 1-arcmin error circle of AX J0105–722 (Yokogawa & Koyama 1998). A study of the region around AX J0105–722 by Filipovic et al. (2000) resolved several sources. Filipovic et al. (2000) proposed that the most likely counterpart to the ASCA source was RX J0105.1–7211. Within errors the *Chandra* source is also consistent with this *ROSAT* PSPC object. A search for the optical counterpart to the ASCA source was carried out by Coe et al. (2005). Based on $H\alpha$ observations and temporal analysis of the $H\alpha$ and optical data, they identified the ASCA X-ray

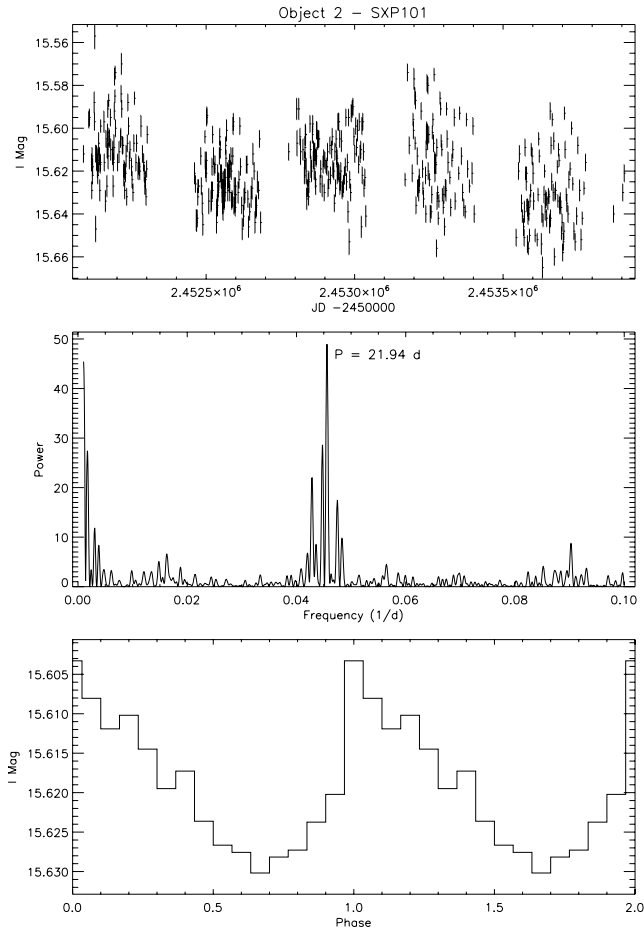


Figure 4. OGLE III light curve (top), Lomb-Scargle periodogram with significant period marked (middle) and folded light curve (bottom) for the optical counterpart of source #2, RX J0057.3–7327 = SXP101. The data have been folded on $P = 21.94$ d using $T_0 = \text{JD } 245\,2124.8625$.

source, designated SXP3.34, with [MA93] 1506 (Meyssonnier & Azzopardi 1993). The position of this optical source also lies within the *ASCA* error circle but it is not consistent with the *ROSAT* or *Chandra* source. A search for pulsations could not be performed on the *ROSAT* data due to poor statistics, and we did not detect any significant pulsations in our search of the *Chandra* data, therefore no firm identification with AX J0105–722 can be made. The *Chandra* position coincides with 2MASS 01050959–7211470 ($J = 16.8$, $H = 16.3$, $K = 15.3$), MACHO object 206.16947.35 ($V = 18.2$, $R = 18.0$) and OGLE III source SMC113.2 13190 ($I = 17.7$). The optical light curves do not show any changes. The X-ray to optical flux ratio is -1.0 , making it difficult to classify the source.

3.10 CXOU J010533.0–721331

This source was detected in observation ID 5486 taken on 2006 February 10 (MJD 53776). The temporal analysis does not reveal any significant periodicities.

The position of CXOU J010533.0–721331 is close to RX J0105.5–7213 (Filipovic et al. 2000). The statistical (90 per cent) positional error of 4 arcsec added in quadrature with the systematic error of 7 arcsec gives an overall positional error of ~ 8 arcsec for RX J0105.5–7213. This error circle encompasses CXOU J010533.0–721331, implying that they are the same source. The

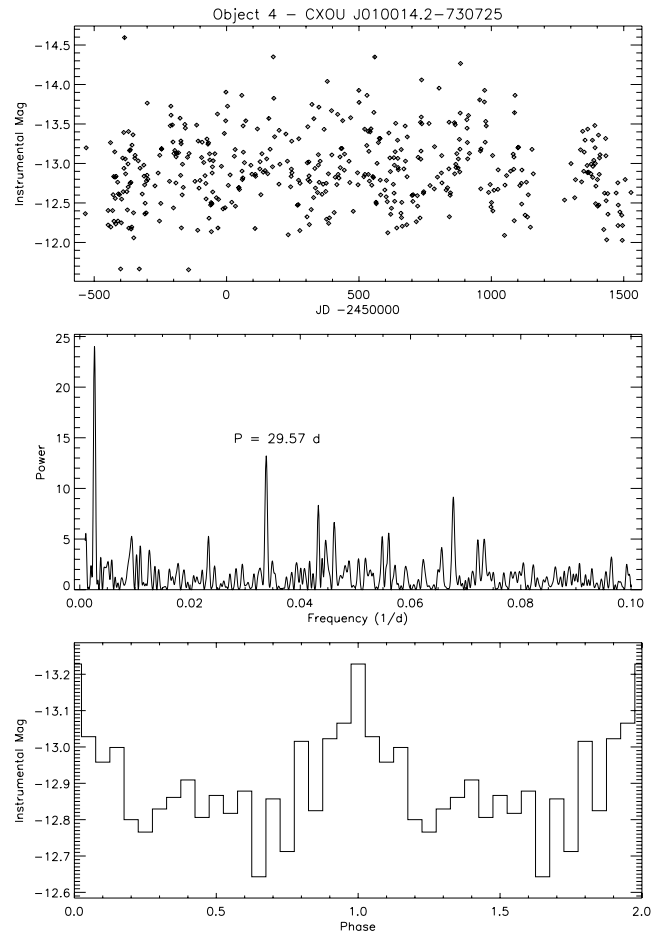


Figure 5. MACHO light curve (top), Lomb-Scargle periodogram with significant period marked (middle) and folded light curve (bottom) for the optical counterpart of source #4, CXOU J010014.2–730725. The data have been folded on $P = 29.57$ d using $T_0 = \text{JD } 245\,0322.5525$.

position of the *Chandra* source coincides with the radio counterpart, J0105.5–7213 (Filipovic et al. 2000), of the *ROSAT* source. Filipovic et al. (2000) did not detect any optical counterpart to this source and classified it as an optically faint background AGNs. However, we find that CXOU J010533.0–721331’s position is consistent with MACHO object 206.16946.1089 ($V = 19.9$, $R = 18.7$) and OGLE III object SMC113.2 13509 ($I = 19.1$), and we propose that this source is the optical counterpart to the radio object. There are no long-term variations in the optical light curves and the X-ray to optical flux ratio is consistent with a background AGN.

3.11 CXOU J010712.6–723533

This source was detected in observation ID 5487 taken on 2006 February 10 (MJD 53776). Timing analysis of this object revealed a period of 65.78 ± 0.13 s with a confidence of >99 per cent (see Fig. 2).

The position of the source coincides with the emission line star [MA93] 1619 (Meyssonnier & Azzopardi 1993). The source is also close to 2E 0105.7–7251 = RX J0107.1–7235 (Kahabka et al. 1999), taking into account the 90 per cent confidence positional uncertainty of 15 arcsec for this source, the position is consistent with CXOU J010712.6–723533 (following the convention of Coe et al. 2005 this source would be designated SXP65.8). 2E 0105.7–7251

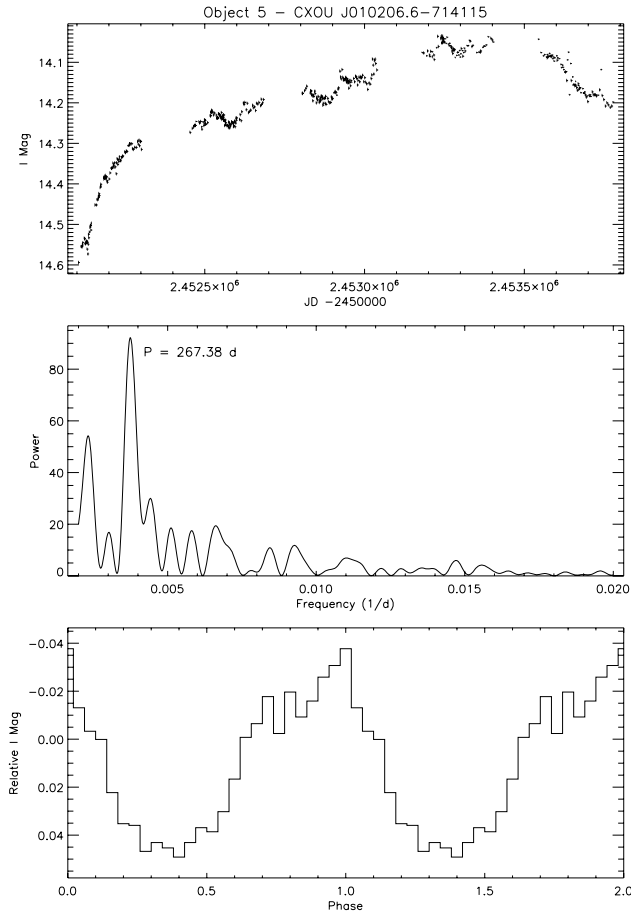


Figure 6. OGLE III light curve (top), Lomb-Scargle periodogram with significant period marked (middle) and folded light curve (bottom) for the optical counterpart of source #5, CXOU J010206.6–714115. The data were detrended using a polynomial before the period search was performed and hence the folded light curve is given in relative I mag. The data have been folded on $P = 267.38$ d using $T_0 = \text{JD } 245\,2264.6099$.

has been identified with a $V = 16.6$ Be star, the $B - V$ colour index is -1.2 . CXOU J010712.6–723533’s position is consistent with 2MASS 01071259–7235338 ($J = 15.8$, $H = 15.4$, $K = 15.2$), MACHO object 206.17055.21 ($V = 15.0$, $R = 14.9$) and the OGLE II source SMC-SC11 48835 ($I = 15.7$). The long-term light curves show a brightening of ~ 0.02 mag over ~ 1200 d, but no periodic modulation is detected. The source falls in a gap between the chips in OGLE III.

We fitted the spectrum of CXOU J010712.6–723533 with a power law and a blackbody, both with photoelectric absorption. Initially we fixed the column density at $6 \times 10^{20} \text{ cm}^{-2}$. This resulted in a best-fitting power law with index 0.3 and unabsorbed luminosity of $3.1 \times 10^{36} \text{ erg s}^{-1}$. Since we detected a high number of counts from this source, we also fitted the column density. In this case the spectrum was again best fit with a power law with index 0.5, $N_{\text{H}} = 1.9 \times 10^{21} \text{ cm}^{-2}$ and an unabsorbed luminosity of $3.0 \times 10^{36} \text{ erg s}^{-1}$ (see Table 2). Statistically the power-law fits cannot be distinguished from each other.

3.12 CXOU J010735.0–732022

This source was detected in observation ID 5496 taken on 2006 March 3 (MJD 53797). The temporal analysis does not reveal any

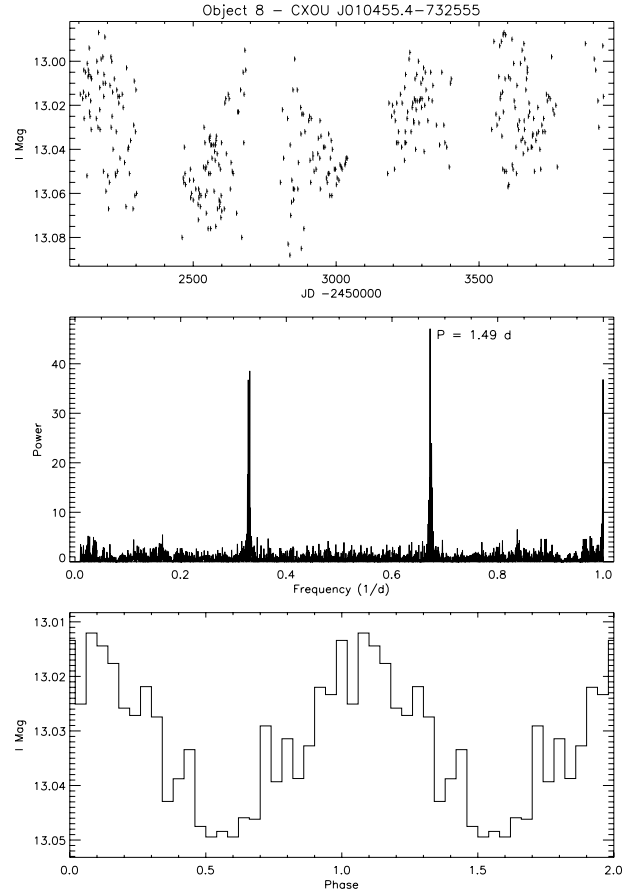


Figure 7. OGLE III light curve (top), Lomb-Scargle periodogram with significant period marked (middle) and folded light curve (bottom) for the optical counterpart of source #8, CXOU J010455.4–732555. The data have been folded on $P = 1.488$ d using $T_0 = \text{JD } 245\,2214.6844$.

significant periodicities. There are no optical or infrared matches for this source.

3.13 CXOU J010836.6–722501

This source was detected in observation ID 5487 taken on 2006 February 10 (MJD 53776). The temporal analysis does not reveal any significant periodicities. The position of CXOU J010836.6–722501 is consistent within errors to the position of source 117 in the ROSAT HRI SMC catalogue (Sasaki et al. 2000). The spectrum of the source was found to be hard (Haberl et al. 2000) and led Sasaki et al. (2000) to classify the source as an X-ray binary or AGNs. The position of the *Chandra* source also coincides with MACHO object 206.17114.1658 ($V = 18.8$, $R = 18.5$), OGLE II source SMC-SC11 116013 ($I = 19.5$) and OGLE III source SMC113.1 9719 ($I = 19.6$). The long-term optical light curve shows a brightening of ~ 0.5 mag over ~ 800 d. As we do not detect pulsations from the source, and taking into account its position on the QCCD compared to the pulsars we have detected and its X-ray to optical flux ratio, we conclude it is likely that this source is a background AGN.

3.14 CXOU J010849.5–721232

This source was detected in observation ID 5485 taken on 2006 February 8 (MJD 53774). The temporal analysis does not reveal any

significant periodicities. The position of CXOU J010849.5–721232 is consistent with the MACHO object 206.17175.739 ($V = 20.3$, $R = 19.4$), the OGLE II object SMC-SC11 120966 ($I = 20.0$) and the OGLE III object SMC118.7 galaxy ($I = 20.5$). The long-term optical light curves do not vary. The X-ray emission from CXOU J010849.5–721232 can be described by a power law with a photon index of 1.7 or with a thermal emission model with temperature 7.4×10^7 K (see Table 2). The temperature is poorly constrained and based on this the non-thermal fit is preferred. In this case the X-ray to optical ratio indicates that the source is a background AGN.

3.15 CXOU J010855.6–721328

This source was detected in observation ID 5485 taken on 2006 February 8 (MJD 53774). The temporal analysis does not reveal any significant periodicities. The position of CXOU J010855.6–721328 coincides with OGLE III source SMC118.7 galaxy and MACHO object 206.17174.524 ($V = 19.5$, $R = 18.9$). There are no changes apparent in the optical light curves and the X-ray to optical flux ratio is consistent with a background AGN.

3.16 CXOU J011021.3–715201

This source was detected in observation ID 5483 taken on 2006 February 6 (MJD 53772). The temporal analysis does not reveal any significant periodicities. Within errors the position of CXOU J011021.3–715201 is consistent with USNO-B1.0 0181–0039286 ($R1 = 19.0$, $B2 = 18.8$, $R2 = 19.1$) and OGLE III source SMC118.5 1160 ($I = 18.8$). The long-term optical light curve shows some variation (~ 0.2 mag) on ~ 100 d time-scales. The X-ray to optical flux ratio implies that the source is a background AGN.

3.17 CXOU J011050.6–721025

This source was detected in observation ID 5484 taken on 2006 February 6 (MJD 53772). The temporal analysis does not reveal any significant periodicities. Within errors the position of CXOU J011050.6–721025 is coincident with the radio source [FBR2002] J011050–721026 (Filipovic et al. 2002) and OGLE III source SMC118.7 10314 ($I = 20.5$). Analysis of the long-term OGLE III light curve does not show any variations. Based on the identification of the *Chandra* source with a radio object suggests CXOU J011050.6–721025 is a background AGN.

3.18 CXOU J011154.2–723105

This source was detected in observation ID 5488 taken on 2006 February 12 (MJD 53778). A peak at 19.52 ± 0.03 s with >90 per cent confidence was detected in the Lomb–Scargle periodogram. A search using Phase Dispersion Minimization does not find a similar modulation.

A tentative detection of an X-ray source, designated BKGS 20, ~ 3 arcsec from CXOU J011154.2–723105 has previously been reported (Bruhweiler et al. 1987). However, a more stringent analysis of the *Einstein* data by Wang & Wu (1992) failed to detect the source. The position of the *Chandra* source is coincident with USNO-B1.0 0174–0065503 ($R1 = 19.3$, $B2 = 18.9$, $R2 = 18.5$) and the OGLE III source SMC115.5 12842 ($I = 19.1$).

The position of the source on the quantile analysis plot is intriguing (Fig. 3); it seems to lie between the detected pulsars and the rest of the sources in our sample. The source shows possible pulsed emission, however the magnitudes of the optical counterpart, and

its lack of variability on long time-scales, indicates that it is not a Be/X-ray transient. In addition, the X-ray to optical flux ratio indicates that the source is a background AGN.

3.19 CXOU J011303.4–724648

This source was detected in observation ID 5490 taken on 2006 February 27 (MJD 53793). The temporal analysis does not reveal any significant periodicities. The position of CXOU J011154.2–723105 is consistent with OGLE III source SMC115.7 18128 ($I = 19.8$), whose light curve exhibits a brightening over ~ 1500 d of ~ 0.4 mag.

3.20 CXOU J011744.7–733922

This source was detected in observation ID 5494 taken on 2006 March 1 (MJD 53795). The temporal analysis does not reveal any significant periodicities. A *ROSAT* PSPC X-ray source has previously been detected near the position of CXOU J011744.7–733922. The archival source, [HFP2000] 537 (Haberl et al. 2000), has a positional uncertainty of ~ 10 arcsec which encompasses the position of the *Chandra* source. This suggests that they are the same object. CXOU J011744.7–733922's position is consistent with USNO-B1.0 0163–0044338 ($R1 = 19.6$, $B2 = 19.5$, $R2 = 19.2$) and OGLE III source SMC117.4 3274 ($I = 18.4$). The OGLE III light curve shows a brightening of ~ 0.4 mag in ~ 1000 d. The X-ray to optical flux ratio implies that the source is a background AGN.

3.21 CXOU J011832.4–731741

This source was detected in observation ID 5493 taken on 2006 February 27 (MJD 53793). The temporal analysis does not reveal any significant periodicities. A *ROSAT* PSPC X-ray source has previously been detected near to the position of CXOU J011832.4–731741. The archival source, [HFP2000] 449 (Haberl et al. 2000), has a positional uncertainty of ~ 9 arcsec which encompasses the position of the *Chandra* source. It is therefore likely that they are the same object. CXOU J011832.4–731741's position coincides with OGLE III source SMC121.6 galaxy, which suggests that it is a background AGN.

3.22 CXOU J012027.3–724624

This source was detected in observation ID 5491 taken on 2005 July 24 (MJD 53575). The temporal analysis does not reveal any significant periodicities. The position of CXOU J012027.3–724624 coincides with OGLE III source SMC120.7 6336 ($I = 20.5$). The long-term optical light curve does not show any variability.

3.23 CXOU J012223.6–730848

This source was detected in observation ID 5492 taken on 2005 August 12 (MJD 53594). A peak with >90 per cent confidence was detected in the Lomb–Scargle periodogram at 140.99 ± 1.50 s, however there is no corresponding strong peak in the Phase Dispersion Minimization periodogram. Analysis of the data with the method used for finding pulsars in *RXTE* data (Galache 2006) reveals a possible periodicity at 282.49 s, approximately twice the value from the Lomb–Scargle periodogram. In this method the light curve is folded on the period found in the Lomb–Scargle to produce a pulse profile. The pulse profile is then used as a template to subtract the pulsations from the light curve. A Lomb–Scargle periodogram is generated for

the cleaned light curve, and this power spectrum is subtracted from the original. The resulting power spectrum shows only the contribution of the pulsar to the Lomb–Scargle, allowing possible harmonics that may have been lost in the noise to be detected.

The position of CXOU J012223.6–730848 is consistent with USNO-B1.0 0168–0053065 ($R1 = 19.1, B2 = 20.8, R2 = 19.3$) and OGLE III source SMC121.4 542 ($I = 18.9$). There are no changes detected in the optical light curves. The X-ray spectrum is described equally well by a power law with photon index 1.5 and a bremsstrahlung with a temperature of 1.1×10^8 K (see Table 2). The temperature is poorly constrained and we therefore prefer the non-thermal fit to the data.

The optical magnitude, lack of long-term variability in the optical light curve and the position of the source on the QCCD (see Fig. 3 and Section 4) suggests that this source may not be a pulsar. The X-ray to optical flux ratio determined using the non-thermal model fit implies that the source is a background AGN. Further observations are needed to verify the existence of pulsations and determine the nature of the source.

4 DISCUSSION

Observations have shown that the SMC contains a large number of HMXBs, providing a homogeneous sample with which to investigate the evolution of the SMC, and to compare with our Galaxy. The HMXBs are tracers of very young populations and the SMC seems to have a particularly prominent young population. To date, studies of the SMC have mostly concentrated on the Bar of the SMC. To obtain a full picture of the history of the SMC we need to broaden our study and include the outer regions of the SMC.

In this first paper from the SMC Wing Survey we have investigated the X-ray and optical characteristics of the 23 brightest X-ray sources. The temporal analysis, combined with identification of the optical counterparts, shows that our sample contains four pulsars, two newly detected and two previously known. The statistical significance of this cannot be determined until a full analysis of the entire SMC Wing Survey has been performed. The other sources include a quasar and possibly two foreground stars. The classifications of the remainder are not conclusive, but the lack of pulsations, long-term periodic variability, optical identifications and X-ray to optical flux ratios imply that they are most likely background AGNs. The classifications of several of the sources from the literature would seem to agree with this. If the preliminary classifications we have presented in this paper are confirmed our results indicate that the spectral hardness and quantile analysis could be used to distinguish between different classes of object (see below).

We have analysed the spectra of the 11 sources that have >100 counts (see Table 2). Apart from source #4, which is probably a variable star, most of the objects exhibit non-thermal emission. We have been able to fit the spectra of all four pulsars in our sample, their power-law indices display a limited range of values with an average of 0.5 and s.d. of 0.2. In comparison, the spectra of the remaining seven sources with >100 counts have softer spectra, with an average photon index of 1.6 ± 0.2 (excluding #4). Haberl & Pietsch (2004) found that the distribution of photon indices for SMC HMXBs, mainly located in the Bar, had an average of 1.0 ± 0.2 . This is in agreement with the Bar pulsars studied by Edge et al. (2004) that have an average photon index of 1.1 ± 0.5 . In general, the pulsars that we have detected in the Wing have harder spectra than those in the Bar.

It is likely that the pulsars have a higher intrinsic neutral hydrogen column density than the AGNs, however it is puzzling why the

Wing pulsars as a group are harder/more absorbed than the Bar group. Could the Wing pulsars be situated at the back of the SMC? The work of Laney & Stobie (1986) would seem to rule out that possibility as they found that the Wing lies in front of the main body of the SMC. It is more likely that small number statistics are contributing to the observed division of sources.

A large fraction of our sources are too faint to extract a meaningful spectrum. By constructing a QCCD we have been able to investigate the spectral properties of all 23 sources in our sample (see Fig. 3). Our analysis shows that the pulsars we have detected in the Wing fall in a distinct group on the QCCD. The location of the Bar pulsars from Edge et al. (2004) also seem to fall in the harder part of the diagram, but the separation of sources is less clearly defined, with one source falling amongst the softer sources from the Wing. There does not seem to be anything remarkable about this particular Wing pulsar. The softer sources include an identified star, quasar and possible AGNs. The source that appears to sit in the transition region between the majority of the pulsars and the other sources is CXOU J011154.2–723105 (source #18). This object displays a possible pulsation of 19.52 s, but its optical magnitude and lack of long-term variability seems to rule out a Be/X-ray transient, and the nature of the source remains unclear.

The classification of all of the sources will require optical spectroscopy, but the QCCD may be a useful tool for distinguishing pulsars from other types of object (stars, quasars, AGNs) for the fainter X-ray sources in the SMC Wing survey.

5 SUMMARY

We have detected two new pulsars, CXOU J010712.6–723533 and CXOU J010206.6–714115, and observed two previously known pulsars, SXP101 and SXP348. With the accurate positions provided by *Chandra* we have been able to determine new optical identifications for the two new pulsars, CXOU J010712.6–723533 and CXOU J010206.6–714115, and SXP101. We have found long-term optical periods of 267 and 21.9 d for CXOU J010206.6–714115 and SXP101, respectively.

ACKNOWLEDGMENTS

AU was supported by the BST grant of the Polish MNSW. RHDC and SL acknowledge support from Chandra/NASA grant GO5-6042A/NAS8-03060. This research has made use of the SIMBAD data base, operated by CDS, Strasbourg, France. This paper utilizes public domain data originally obtained by the MACHO Project, whose work was performed under the joint auspices of the US Department of Energy, National Nuclear Security Administration by the University of California, Lawrence Livermore National Laboratory under contract no. W-7405-Eng-48, the National Science Foundation through the Center for Particle Astrophysics of the University of California under cooperative agreement AST-8809616, and the Mount Stromlo and Siding Spring Observatory, part of the Australian National University.

REFERENCES

- Alcock C. et al., 1999, *PASP*, 111, 1539
- Bruhweiler F. C., KlingleSmith D. A. III, Gull T. R., Sofia S., 1987, *ApJ*, 317, 152
- Cash W., 1979, *ApJ*, 228, 939
- Cioni M.-R. L. et al., 2003, *A&A*, 406, 51
- Coe M. J., Orosz J. A., 2000, *MNRAS*, 311, 169

- Coe M. J., Edge W. R. T., Galache J. L., McBride V. A., 2005, *MNRAS*, 356, 502
- Corbet R. H. D., 1986, *MNRAS*, 220, 1047
- Dobrzycki A., Macri L. M., Stanek K. Z., Groot P. J., 2003, *AJ*, 125, 1330
- Edge W. R. T., Coe M. J., 2003, *MNRAS*, 338, 428
- Edge W. R. T., Coe M. J., Galache J. L., McBride V. A., Corbet R. H. D., Markwardt C. B., Laycock S., 2004, *MNRAS*, 353, 1286
- Edge W. R. T. et al., 2005, *MNRAS*, 361, 743
- Filipovic M. D. et al., 1998, *A&AS*, 127, 119
- Filipovic M. D., Haberl F., Pietsch W., Morgan D. H., 2000, *A&A*, 353, 129
- Filipovic M. D., Bohlsen T., Reid W., Staveley-Smith L., Jones P. A., Nohejl K., Goldstein G., 2002, *MNRAS*, 335, 1085
- Galache J. L., 2006, PhD thesis, Univ. Southampton
- Gardiner L. T., Noguchi M., 1996, *MNRAS*, 278, 191
- Grimm H.-J., Gilfanov M. R., Sunyaev R. A., 2003, *MNRAS*, 339, 793
- Haberl F., Pietsch W., 2004, *A&A*, 414, 667
- Haberl F., Filipovic M. D., Pietsch W., Kahabka P., 2000, *A&AS*, 142, 41
- Hong J., Schlegel E. M., Grindlay J. E., 2004, *ApJ*, 614, 508
- Hong J., van den Berg M., Schlegel E. M., Grindlay J. E., Koenig X., Laycock S., Zhao P., 2005, *ApJ*, 635, 907
- Horne J. H., Baliunas S. L., 1986, *ApJ*, 302, 757
- Hornschemeier A. E. et al., 2001, *ApJ*, 554, 742
- Hughes J. P., Smith R. C., 1994, *AJ*, 107, 4
- Israel G. L., Stella L., Campana S., Covino S., Ricci D., Oosterbroek T., 1998, *IAUC*, 6999, 1
- Israel G. L. et al., 2000, *ApJ*, 531, 131
- Kahabka P., Pietsch W., Filipovic M. D., Haberl F., 1999, *A&AS*, 136, 81
- Kennicutt R. C. Jr, 1991, in Haynes R. F., Milne D. K., eds, *Proc. IAU Symp.* 148, *The Magellanic Clouds*. Reidel, Dordrecht, p. 139
- Kovács G., 1981, *Ap&SS*, 78, 175
- Laney C. D., Stobie R. S., 1986, *MNRAS*, 222, 449
- Laycock S., Corbet R. H. D., Coe M. J., Marshall F. E., Markwardt C., Lochner J., 2005, *ApJS*, 161, 96
- Maccacaro T., Gioia I. M., Wolter A., Zamorani G., Stocke J. T., 1988, *ApJ*, 326, 680
- Massey P., 2002, *ApJS*, 141, 81
- Mennickent R. E., Pietrzynski G., Gieren W., Szewczyk O., 2002, *A&A*, 393, 887
- Meyssonier N., Azzopardi M., 1993, *A&AS*, 102, 451
- Nazé Y., Hartwell J. M., Stevens I. R., Manfroid J., Marchenko S., Corcoran M. F., Moffat A. F. J., Skalkowski G., 2003, *ApJ*, 586, 983
- Sasaki M., Haberl F., Pietsch W., 2000, *A&AS*, 147, 75
- Schmidtke P. C., Cowley A. P., 2006, *AJ*, 132, 919
- Shtykovskiy P., Gilfanov M., 2005, *MNRAS*, 362, 879
- Stanimirović S., Staveley-Smith L., Dickey J. M., Sault R. J., Snowden S. L., 1999, *MNRAS*, 302, 417
- Szymański M. K., 2005, *Acta Astron.*, 55, 43
- Torii K., Kohmura T., Yokogawa J., Koyama K., 2000, *IAUC*, 7441, 2
- Tucholke H.-J., De Boer K. S., Seitter W. C., 1996, *A&AS*, 119, 91
- Udalski A., Kubiak M., Szymański M., 1997, *Acta Astron.*, 47, 319
- Wang Q., Wu X., 1992, *ApJS*, 78, 391
- Westerlund B., 1997, *The Magellanic Clouds*. Cambridge Univ. Press, Cambridge
- Yokogawa J., Koyama K., 1998, *IAUC*, 7009, 3

This paper has been typeset from a $\text{\TeX}/\text{\LaTeX}$ file prepared by the author.